Available online at www.sciencedirect.com

SciVerse ScienceDirect

Physics Procedia 26 (2012) 261 – 273

Physics Procedia

Union of Compact Accelerator-Driven Neutron Sources I & II

Status of the LEgnaro NeutrOn Source facility (LENOS)

Pierfrancesco Mastinu*[a], J. Praena[b], G. Martín-Hernández[c], N. Dzysiuk[a], G. Prete[a], R. Capote[d], M. Pignatari[e], A. Ventura[f]

[a] *INFN, Laboratori Nazionali di Legnaro, Italy*
[b] *Universidad de Sevilla, CNA, Sevilla, Spain*
[c] *Centro de Aplicaciones Tecnológicas y Desarrollo Nuclear,La Habana, Cuba*
[d] *NAPC-Nuclear Data Section, International Atomic Energy Agency, Vienna, Austria*
[e] *Department of Physics, University of Basel, Switzerland*
[f] *ENEA, Bologna and INFN Sezione di Bologna*

Abstract

LENOS is a new facility under development at Laboratori Nazionali di Legnaro (LNL). It is based on a new technic for neutron beam shaping in accelerator based neutron sources. The main advantage of this method is to be able to shape the primary charged-particle beam to a defined energy distribution that, impinging on a neutron producing target, generates the desired neutron spectra at the sample position. Together with the proton energy distribution, other degrees of freedom are used to obtain the desired neutron energy spectra, e.g. the angular distribution of produced neutrons, the nuclear reactions used for the neutron spectra production, and the convolution of neutron spectra coming from different target materials. The main advantage of this new approach is the good control over the energy and spatial distribution of the produced neutron spectrum avoiding most of the problems due to neutron moderation, since it is easier to work with charged particles than with neutrons. The goal of the LENOS facility is to obtain a Maxwell-Boltzmann neutron energy spectrum with tunable temperature and a high neutron flux at sample position by using the ^{7}Li(p,n) reaction. To maximize the neutron flux a very narrow primary proton beam has to be used, so the target has to remove a very high specific power. Currently available lithium targets are inadequate to sustain the high specific power that needs to be dissipated in the LENOS facility. A dedicated target based on micro-channel geometry and liquid metal cooling has been developed and tested. This contribution describes the status of the LENOS facility.

Keywords: Nuclear astrophysics; neutrons; irradiation facility; neutron activation; benchmark validation

*Corresponding author: Tel: +39 049 8068 434 (683)
E-mail address: Pierfrancesco.Mastinu@lnl.infn.it

1875-3892 doi:10.1016/j.phpro.2012.03.034

1. Introduction

In the last years a renewed interest in low energy neutron physics has triggered the construction of new facilities as well as many experimental apparatus. This process has been mainly boosted by the needs of nuclear data in several fields like nuclear astrophysics, nuclear waste transmutation, generation IV reactors, accelerator-driven-systems, fusion reactors, decommissioning of first generation fission reactors, radioprotection, medical physics, dosimetry and material science.

The LENOS facility is under development at Laboratori Nazionali di Legnaro of the INFN in the framework of the SPES and TRASCO projects. It is based on a new method and a novel lithium target proposed in [1]. It would be the first high level accelerator-based neutron facility for basic and applied research in Italy. The main goal of the facility is to provide new and more accurate neutron cross sections data of interest in the above-mentioned fields. Additional motivation is the possibility to measure integral nuclear data in a very well characterized broad beam neutron spectra. Such data are very important for benchmarking of available nuclear data files in the unresolved resonance and fast neutron ranges.The present paper is focused on radiative neutron capture cross section (n,γ) measurements, although measurements of neutron induced charged-particle emission cross section with applications to nuclear astrophysics and fusion technology, are also feasible and will be investigated in the future. The paper is organized as follows: the physics cases related to astrophysics and validation of nuclear data are presented in section 2; section 3 contains a brief summary of the method; the target and the power test performed are described in section 4; and the prospective of the facility is given in section 5. Finally, conclusions are reported in section 6.

2. Motivations

2.1. Radiative capture: nuclear astrophysics

The nucleosynthesis of the elements beyond ^{56}Fe is produced in stars mainly by the slow neutron capture process (called s process) and the rapid neutron capture process (r process), which basically consist of successive neutron-captures and β-decays [2,3]. In particular, the s-process is characterized by low neutron densities ($n_n \lesssim 10^{11}$ cm^{-3}) where the neutron capture time scale is usually lower than the β-decay rate for unstable species, forcing the s-process path to advance along the valley of stability [4,5,6,7,8]. On the other hand, the r-process is characterized by high neutron densities ($n_n \approx 10^{20}$ cm^{-3}), with neutron capture time scale faster than β-decay. The neutron capture cross sections (NCCS) of isotopes involved in neutron capture processes in stars are the fundamental ingredient for robust nucleosynthesis calculations, and for obtaining reliable stellar abundance yields to compare with observations. To reproduce the solar system distribution of the s-process abundances, three components are required: the weak s-process component (hosted by massive stars, responsible for most of the s-process abundances between Iron and Strontium) [4,5], the main s-process component (hosted by low mass Asymptotic Giant Branch-AGB) stars at solar-like metallicity and mostly efficient production between the Strontium and Lead neutron magic peaks [6,7] and the strong s-process component (hosted by low mass AGB stars at low metallicity, and producing e.g., half of the solar ^{208}Pb) [7,8].

The wide neutron density regime between s-process and r-process is experienced in both low mass stars and massive stars. For instance, during thermal pulses in low mass low mass AGB stars, the ^{22}Ne(α,n)^{25}Mg activation causes neutron densities of ~ few 10^{11} cm^{-3} [9] or in massive stars the same reaction may generate neutron densities up to few 10^{12} cm^{-3} in convective C-burning shell [10].

In other cases, the nucleosynthesis signature of non-standard neutron capture processes is directly observed (e.g., the post-AGB Sakurai object, where its surface abundances were likely affected by neutron densities up to $10^{14\text{-}15}$ cm^{-3}) [11], or measured in presolar stellar dust, relic of dead stars trapped in carbonaceous meteorites (e.g., silicon carbide or SiC X grains from massive stars, showing the signature of a neutron burst of $\sim 10^{18}$ cm^{-3} occurring during the core collapse supernova in the explosive He shell) [12].

Reliable stellar nucleosynthesis calculations require a precise knowledge of NCCS to use in astrophysical networks, able to handle such a large spread of stellar conditions, characterized by different neutron densities and different temperatures.

A branching point is a particular case in the s-process path that corresponds to an unstable isotope with a β-decay probability comparable with the probability of neutron capture, e.g. ^{79}Se, ^{85}Kr, ^{151}Sm and ^{153}Gd nuclei [13].

Their astrophysical relevance is due to the fact that their behavior is sensible to the stellar environment (e.g., temperature, neutron density, matter density), and the resulting nucleosynthesis of neighbor species is affected. Therefore, such abundances may provide an indirect observation of stellar conditions where neutron capture process is activated. For these isotopes, mainly theoretical neutron capture cross sections are usually available and their uncertainty is about a factor of 2-3 according to the spread of predictions from nuclear theoretical models.

In stellar sites where neutron capture processes take place, neutrons are quickly thermalized and exhibit a Maxwell–Boltzmann spectrum corresponding to the stellar temperature or stellar thermal energy kT typical of the mass and evolutionary stage of the star. For the s-process the most important stellar thermal energies are 8, 23 and 90 keV, being 30 keV the reference stellar temperature.

The astrophysical reaction rates during the shell burning phases can be calculated from the Maxwellian averaged cross section (MACS) defined as,

$$MACS = \frac{\langle \sigma v \rangle}{v_T} = \frac{2}{\sqrt{\pi}} \frac{\int_0^\infty \sigma(E_n) E_n e^{-E_n/kT} dE_n}{\int_0^\infty E_n e^{-E_n/kT} dE_n} \qquad (1.1)$$

Where T is the temperature and σ(En) the energy-dependent neutron capture cross section. The MACS can be calculated analytically at every stellar temperature using the cross section as a function of neutron energy, see [12] Because of the necessary neutron flight path and duty cycle in such measurements, the flux at the sample position is several orders of magnitude lower than at the source. This implies a severe limitation for the required sample mass (as in the case of radioactive samples). If samples of a few micrograms or less have to be used, the only alternative are, when feasible, activation measurements, which can be performed in a much higher neutron flux placing the sample in touch with the neutron source.

However, to measure the MACS by activation, the neutron spectrum should correspond to the thermal distribution of the stellar environment. So it is needed to produce a Maxwell–Boltzmann neutron spectrum (MBNS) at the stellar temperatures of interest. Up to now, most of the accurate MACS have been calculated at one stellar temperature (at kT=25 keV) by making corrections from a direct activation measurement with a neutron spectrum similar to a MBNS at kT=25 keV. The most important MACS measurements by activation have been done by using the method of [15] and [16] based on the known properties of the 7Li(p,n) reaction near the threshold (1.881 MeV). They were able to generate a neutron spectrum similar to a MBNS at kT=25 keV by impinging a 1.912 MeV proton beam onto a thick lithium target. With this spectrum the authors of ref [12,13] calculate the MACS at kT=30 keV applying two corrections to the experimental data: one associated with the lack of neutrons from 100 to 250 keV; second the extrapolation from 25 to 30 keV is done assuming the knowledge of

the behaviour of the cross section as a function of the energy. With the LENOS method it would be possible to measure by activation directly the MACS at several kT's, without or with reduced corrections to the experimental data.

Another exciting challenge of the LENOS project is the possibility of a direct measurement of the MACS of radioactive isotopes (like the branching points) using the unique possibility of having in situ both the Radioactive Ion Beam (RIB) of the SPES project and the shaped neutron beam with high flux of LENOS facility. For the major part of these radioactive isotopes there are no data so, even a measurement with large uncertainty could be very useful. The idea is to implant a radioactive species onto a substrate (for instance graphite) to create the sample, and then the radioactive sample would be irradiated with the Maxwell-Boltzmann neutron spectrum beam of LENOS. Many technical aspects must be evaluated to verify the feasibility of such kind of measurements, as the best MBNS energy and RIB (Radioactive ion Beam) flux. Nevertheless some preliminary calculations have been done for some isotopes of interest for astrophysics and scheduled to be produced by SPES.

2.2. Radiative capture: other applications

The measurements of radiative neutron capture cross sections that could be performed at LENOS facility are of interest in other fields such as basic nuclear physics and validation of nuclear data for different applications.

Presently, nuclear reaction theory produces a qualitative nuclear data (cross sections, nuclear structure) being the models and the associated computer codes the core elements of the data generation. There is no one universal nuclear reaction model able to describe the reaction process at all its stages. Several codes had been developed over years; e.g. two representative codes of the latest generation are TALYS [17] and EMPIRE [18] systems. These new codes are designed to automatically retrieve the recommended set of input parameters mostly from the RIPL database [19], allowing for a default calculation with a minimum input. Those input parameters also include a large nuclear structure data library. These codes contain an implementation of various theoretical models of a nuclear reaction, the most important being the optical model, the Hauser-Feshbach statistical model including the fission decay, and pre-equilibrium models. The nuclear reaction theory used in theses codes could be verified and improved by comparing results of calculations vs. experimental data measured in a very well characterized conditions, as those provided by LENOS facility.

On the other hand, there are compelling needs for nuclear data also for many fields of applied nuclear physics and, in particular, those related to the production of nuclear energy. Calculations undertaken with modelling codes are combined with available differential data measurements to produce evaluated nuclear data files (e.g. recently released JEFF-3.1.1 [20], JENDL4.0 [21] and ENDF-B/VII.1 [22]). The processed data libraries derived from the evaluated data libraries constitute the backbone of input data for Monte Carlo transport codes as MCNP [23] and GEANT [24]. Therefore, the predicted accuracy of radiation transport undertaken by Monte Carlo codes critically depends on the accuracy of data in evaluated nuclear databases. The validation of evaluated nuclear data files requires availability of accurate integral data measured in broad neutron spectra. A series of integral activation measurement could be performed at LENOS facility providing a new comprehensive experimental data set for validating important for applications evaluated nuclear data files.

3. The LENOS method

The general method consists in shaping the primary charged particle beam to a distribution or to a convolution of distributions that, impinging on a neutron producing target generates the desired neutron spectrum at the sample position.

Figure 1 shows a sketch of the layout needed to apply the LENOS method to the RFQ of the SPES projects, more details can be found in [1]. The charged particle beam is shaped by means of what we call beam shaper. This system includes the foil (or a rotating shaper of different materials and thicknesses), the bending magnet, choppers and all other equipment needed to have the desire beam energy distribution. The shaped beam impinges directly on the neutron producing target, and the sample could be placed at a suitable distance in order to cover the desired angular aperture. The present paper is focused on proton beam and lithium as neutron production target. Figure 1 shows the expected neutron spectrum (black line) and the comparison with a Maxwellian at kT=30 keV. It should be noticed that the agreement between them is very good but an experimental confirmation it is needed, although our simulations are based on experimental data of the ^{7}Li(p,n) reaction, more details in [1].

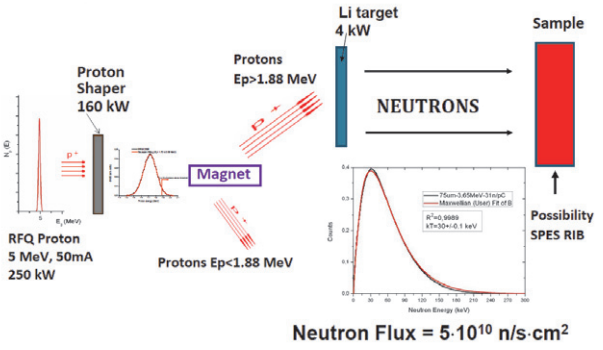

Figure 1 Sketch of the LENOS layout in case of the RFQ of the TRASCO and SPES projects. The simulated neutron spectrum at the sample position (black line) is compared with a Maxwellian at kT=30 keV.

However the LENOS method is more general and flexible and is possible to generate MBNS at kT=30 keV (and other kT) in different ways considering proton beam of lower energy and current as shown in section 5.

4. The LENOS target

The LENOS project has been designed to develop an intense neutron source to be used in neutron activation analysis for nuclear astrophysics, nuclear technology and other fields of nuclear physics in which the neutron activation is of interest. When measuring rare elements or radioactive isotopes the mass of the sample is usually very small. To obtain a high enough number of activated species to achieve the statistical limit imposed by the theory a high neutron flux at sample is required. This can be achieved by increasing the accelerator current, reducing the beam spot size and placing the sample as close as possible to the source.

The proposed neutron producing reaction is ^{7}Li(p,n)^{7}Be because of neutron spectra consideration discussed in [1]. The major drawback of this reaction is that metallic Lithium has a low melting point

of 182 ^{0}C. The factors mentioned above to attain the required neutron fluence rate can be reached if a high-power-dissipating low-mass target is developed. A lithium target cannot be formed only by the Lithium metal, as it is done for other metals and materials, due to its mechanical and chemical properties. Lithium is a very reactive metal, forming lithium oxide immediately upon exposure to air. Also its thermal conductivity and tensile strength are very low [25]. Lithium targets are thus formed by attaching a Lithium layer to a backing material.

In case of the LENOS facility, the dimension of the proton beam should be around 1 cm^2 (smaller is of course even better), so a very high specific power has to be dissipated by a target which melts at 180ºC. Common heat dissipation systems are inadequate for our needs because they are not able to remove so high specific power and/or are too massive. In order to overcome this drawback, we have designed a copper backing where the metal lithium layer is deposited on its surface and particular care has been devoted to the cooling of the backing. In a conceptual study a target structure is usually composed of 3 sections. The first one is the layer deposition (the material we intend to irradiate) of specific deep that is attached to the second section, the backing. The second section is then in touch or immersed in the third one, the cooling fluid. Figure 2 shows schematically the concept of the target.

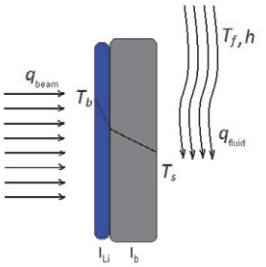

Figure 2: *Target concept.*

T_b *:* temperature on beam side
T_s*:* temperature on fluid side
l: target (backing) thickness
q_{beam}*:* heat flux on beam side
q_{fluid}*:* heat removed by fluid
T_f *:* fluid temperature
h: film coefficient

The fluids with best performance for LENOS purposes are the liquid metals. Liquid metals are an attractive heat transfer fluid for high power density device cooling primarily due to the high thermal conductivity of the material relative to common coolant alternatives. The high thermal conductivity of this class of materials allows energy to efficiently pass from the solid heat transfer surfaces of the source to the cooling fluid. In Table 1 summarizes the thermo physical properties of several liquid metals as well as water for comparison.

Table 1. Summary of the thermophysical properties of liquid metals used in heat transfer applications and water for comparison

	Hg	$Ga_{68}In_{20}Sn_{12}$	$Na_{27}K_{78}$	SnPbInBi	Water
Density (kg/cm^3)	13564.0	6363.2	868.2	9230	998.0
Melting point (ºC)	-38.87	10.5	-11	58	0
Heat capacity (J/(kg·K))	139.068	365.813	982.1	209	4181
Kinematic viscosity (10^{-6} m^2/s)	0.114	0.348	1.05	4.04	0.960
Electrical conductivity (S/μm)	14.044	3.307	2.878	1.25	$5.5\cdot10^{-12}$
Thermal conductivity (W/(m·K)	8.716	39	21.8	10	0.606
Prandtl number	0.024	0.020	0.0411	0.7793	6.62

The main difference between the metals and the other cooling media is that they have a significantly higher thermal conductivity even if a lower specific heat capacity. The thermal conductivity combined with the specific heat capacity can be compressed in Prandtl number which, together with Nusselt number, enter in the definition of the film *h* coefficient. In order to increase the heat removal efficiency, the film *h* coefficient has to be maximized. Ga-In-Sn alloy is a commercially available as Indalloy 46L and is the alloy we are investigating for LENOS as a cooling media.

Together with a proper choice of the cooling medium, the geometry of the target is another task that should be optimized in order to maximize *h*. Since the goal of the target is the dissipation of high power keeping the surface temperature of the target very low, the micro channels configuration appear, for us, the best choice, according to Figure 3 [26]. Using both microchannels and liquid metal increase greatly the Nusselt number (*Nu*) and thus the film coefficient (*h*).

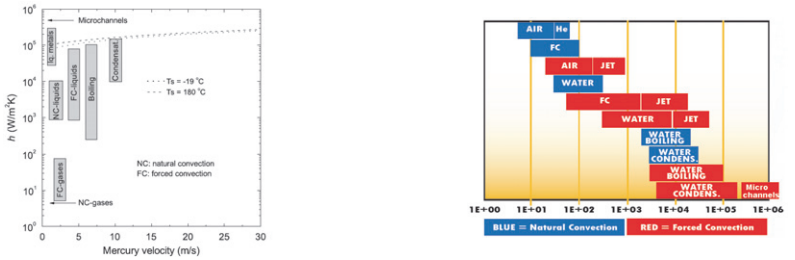

Figure 3 Right: Heat transfer coefficients *h* (W/m^2·K) for some common fluids and different modes. Left: Calculated film convection coefficient as a function of the fluid velocity for a tube of 0.7 mm diameter and two different surface temperatures.

4.1. Target core

The target core was designed and constructed from a solid piece of Copper UNSC15720 by EDM drilling of consecutive holes of 0.5 mm diameter and 15 mm length as shown in the Figure 4. The proton beam is represented in the figure as the heat source and impinges on the Li layer (not visible in the figure). The cooling fluid enters from right to left removing the heat by forced convection. With such a device, FEM calculations shows that a power of 4 kW produced by 1.2 cm diameter beam can be removed using the 46L alloy liquid metal, keeping the surface temperature below 150 ºC.

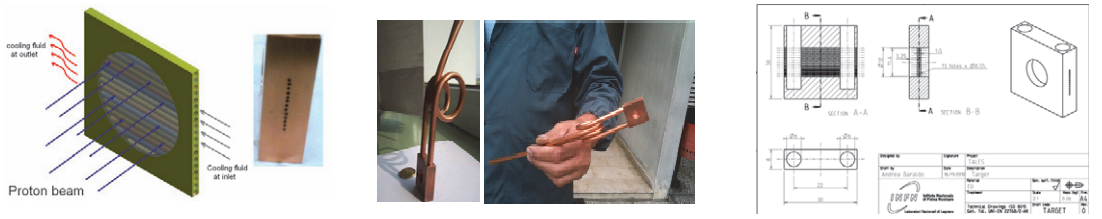

Figure 4 From left to right, target core concept, picture of the prototype showing the micro channels, picture of the assembled prototype compared with a coin, picture of the prototype showing the hole for lithium deposition and technical design of the target.

Figure 4 shows a picture of the target, produced using a copper backing and making the micro channel holes done with electro-erosion drilling machine. The thicknesses of the wall (the distance between the face where the lithium has to be deposited and the inner part of the micro channel), together with the channel-to-channel distance are limited by the performance of the drilling machine (other methods for the production of the target are under development). With our drilling machine, we have been able to make holes of 0.45 mm diameter, with a channel-to-channel distance of 1 mm and a wall thickness of 0.45 mm for a 30 mm long micro channel.

4.2. Target test and FEM calculations

We have performed, recently, tests with water as a cooling medium, since our plan is to implement the metal cooling system in the year 2012. First we have performed an static test (thermo-mechanical test). The target has been heated up to 200 ºC with an internal static pressure of 9 bar and kept in an oven for 5 hours; at the end we have checked the absence of any leak due to the thermal and mechanical stress, as confirmed by a more precise leak test done successively with a sniffer. Since the target is a new design, a beam target test has to be performed carefully, because of the water circulating in the target and the problems related with the beam profile and vacuum. So we have performed a test on air, using a TIG (Tungsten Inert Gas) welding machine to mimic the beam spot. Figure 5 shows the experimental setup. The TIG electrode has been placed close to the centre of the target, two thermocouples measures the temperature of water in and water out and a mass flow meter already calibrated measure the mass flow. The most difficult issue for this configuration is the measurement of the temperature reached by the surface, A direct measurement with some kind of thermometer is not possible, because the arc of the TIG would heat the probe directly, perturbing the

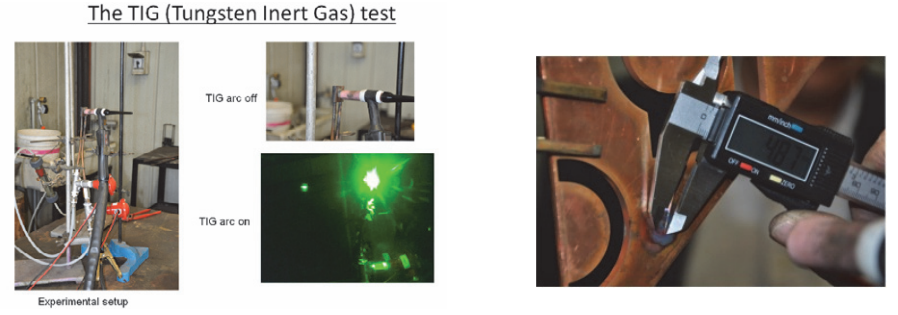

Figure 5 Left: three pictures of the set up of the TIG test. Right: measurement of the TIG beam spot

measurement. Since we need that the surface temperature does not exceed 150 ºC, we have deposited a small layer of Indium. Indium has a thermal conductibility close to that of lithium and a lower melting temperature (150 ºC). Thus, we used the indium deposit as a threshold probe for the surface temperature: if the Indium layer melts the temperature exceeds 150 ºC, otherwise it is below the working temperature of the lithium target.

The maximum transferred power from the TIG to the target has been measured by the difference of temperature of water at inlet and outlet and has been calculated to be 3.4 kW. No melting of indium has been observed for this power. Moreover, the power transferred to the target is mostly superficial with the TIG. This situation is worse than the real case where the proton beam penetrates more into the target backing. Using the adequate mask, we have checked that the TIG spot was much smaller than the beam aperture hole. We also have tried to measure the TIG spot by using a piece of copper not

cooled and flashing a TIG impulse on it. Figure 5 shows the obtained TIG spot and the Calibre gives a measure of the spot. It is much less than 1 cm^2, suggesting that the target is able to remove more than 3.4 kW/cm^2 specific power keeping the surface temperature below 150 ºC.

The result obtained with TIG test is much more favourable than the Finite Element Method (FEM) calculations performed, some of them reported in [1], suggesting that the modelling of micro channel is a complicated task. Figure 6 reports the results of FEM calculations with temperature distribution for 1 kW/cm^2 applied to the surface, using both water and the eutectic alloy of Indium, Tin and Gallium as a cooling media. From FEM calculations (performed with ANSII and CFX package), we expect an increase of performance moving from water to liquid metal of about a factor of 3, suggesting a specific power of about 9 kW/cm^2 as a best performance reachable from the target.

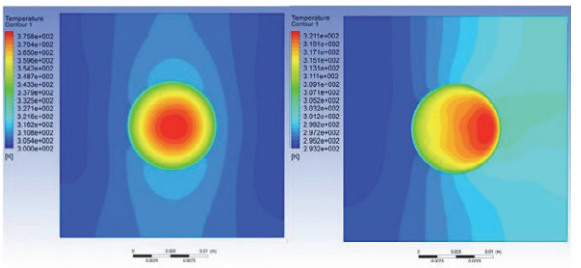

Figure 6 FEM calculations of the temperature surface of the target in case of water cooling (left) and GaInSn alloy (right).

In order to have experimental evidence of the behaviour of our target in terms of heat removal capacity, we have performed a test of the target using also an electron beam, provided by the PATON Institute (Kiev, Ukraine). The target core has been placed in a vacuum chamber at 10^{-4} mm and heated with an electron beam of 60 kV and a maximum current of 74 mA. The temperature distribution of the surface of the target has been acquired with a thermo camera (model IRISYS IRI 4000 series) with a value of the emissivity of 0.84 (the emissivity of the oxidize copper) and reported in Figure 7. As with TIG test, the power delivered to the target has been measured by the difference of temperature of water at inlet and outlet. Data at different power have been collected and a curve of specific power as a function of maximum temperature has been calculated. The calculated value of the temperature is emissivity dependent and the emissivity also depends on temperature. A preliminary calibration of the thermo camera was performed for this test but in order to be sure of the calibration another test is on the way at ENEA Brasimone (Italy), where it is possible to use self designed RF inductor to heat the target. Because of the low efficiency of the system, we expect to deliver to the target a specific power lower than 1.5 kw/cm^2, but the results will allow normalizing correctly the curve obtained at higher power with the electron welding test.

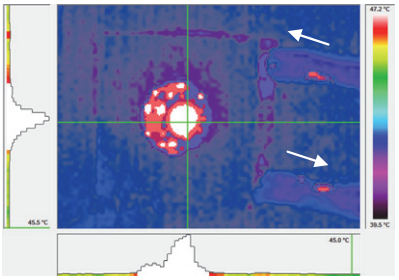

Figure 7 Picture of the cooper backing based on micro channels obtained with the thermo camera at the moment the electron gun was delivering 60 kV and 74 mA. White arrows indicate the entrance and exit of the water cooling Left: three pictures of the set up of the TIG test. Right: measurement of the TIG beam spot

5. LENOS perspectives and current measurements

The LENOS project deals with the RFQ at 5 MeV, 50 mA current under construction within the SPES project at the LNL, but the method we are proposing can also be better used at existing accelerators. Since existing accelerators have much lower current, most of the technical issues related to the dissipation of power can be circumvented and other degrees of freedom (as the variable proton energy and particle type) can be used to better shape the beam energy distribution. Waiting for the construction of LENOS, we are arranging some experiments related with the project: activation measurements at the Tandem 3 MV at CNA (Seville, Spain) and at the CN Van der Graaf accelerator at Legnaro (LNL-INFN, Italy) as well as TOF measurements at IRMM (Geel, Belgium) and the current development of TOF system at CN-LNL.

As pointed out in Section 3, a direct measurement of the Maxwellian neutron spectrum is needed to validate our method. For this purpose, a stellar temperature can be used, even if we plan to measure all spectra relative to the thermal energy we will use for activation measurements; we submitted a proposal to the EUFRAT European project and our proposal was approved *"A new method for the generation of Maxwell-Boltzmann neutron spectra"* (PAC 3/11) [27] and scheduled for the end of March 2012. We are also working in a TOF setup at CN-LNL in order to have 2 ns pulsed beam at tuneable repetition rate.

We have performed so far two activations experiments at CNA, Seville, Spain. Additional experiments at CN-LNL, Italy are in the planning stage. We have evaluated different setups aiming to produce high quality Maxwell-Boltzmann distributions at different kT with a good neutron yield. Because of the low power dissipated in these accelerators, the beam energy shaper consists of a static thin foil of aluminium. In the first activation experiment we have measured the ratio of the MACS of ^{181}Ta to 197Au at kT=35 keV (see more details in Ref. [28]). In the second activation experiment we have measured the ratio of the MACS of ^{181}Ta to ^{197}Au at two different stellar energies kT=30 keV and 55 keV. Remarkable, the tuning of the MACS energy in these two experiments was achieved by changing the incident proton energy only. The thickness of the aluminium foil used as energy shaper was 75 μm. Figure 8 shows the expected neutron spectra in comparison with calculated Maxwellian at kT=30 and 55 keV. In the simulations we have considered the geometry, dimensions and materials of the chamber, samples and experimental hall. Figure 8 on the left shows the expected neutron spectrum passing through the front face of the gold sample (black line) and the red line is a Maxwellian fit at

kT=30 keV. This figure also shows the neutron spectrum passing through the back face of the tantalum sample (blue line) and the corresponding red line is the Maxwellian fit. It should be noticed that the dimension of the samples, and thus the distance from the neutron source could modify the neutron spectrum. In this case the modification is negligible. Figure 8 on the right corresponds to the kT=55 keV activation. A preliminary data analysis provides 837 mb and 462 mb for the MACS of ^{181}Ta at kT=30 keV and 55 keV, respectively, if we take the monitor MACS of ^{197}Au at 30 keV from Ref. [13], and at 55 keV of Kadonis data base [29].

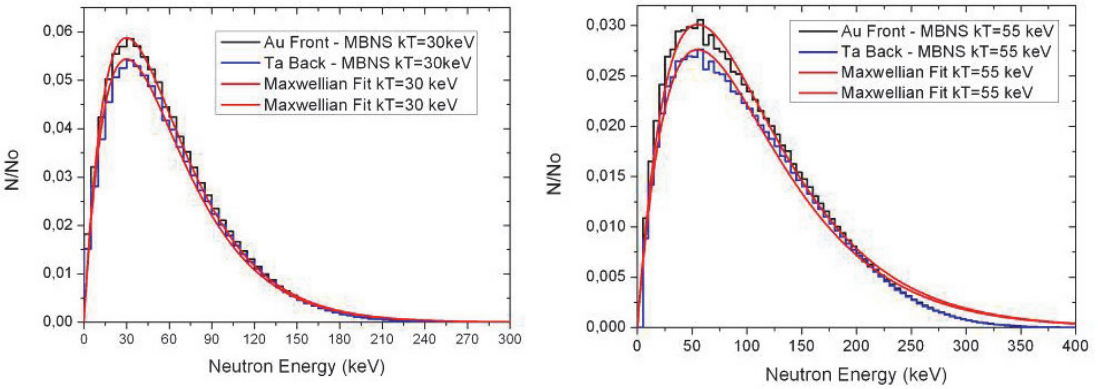

Figure 8 Expected neutron spectra in the second activation experiment performed at Tandem 3 MV at CNA. Left: black histogram is the simulated neutron spectrum passing through front face of the gold sample, the corresponding red line is a Maxwellian fit at kT=30 keV. Blue histogram and the corresponding red line correspond to the back face of the tantalum sample. Right: the same for the activation measurement at kT=55 keV.

Aside from activation experiments we are studying other degrees of freedom of the method, e.g. the position of the sample relative to the neutron production target. Taking advantage of the angular distribution of the ^{7}Li(p,n) reaction it should be possible to generate Maxwellian spectra at different temperatures. Figure 9 summarizes a calculation performed with the procedure outlined in Ref. [1], considering the following degrees of freedom: the proton beam energy, the foil thickness, and the angular aperture of the neutron beam with respect to the proton beam direction. It is shown that with such simple setup, it should be possible to produce high quality Maxwellian neutron distribution facing the measuring target with tunable thermal energy from kT=30 to 60 keV. A slightly lower quality Maxwellian distribution can be achieved increasing much more the neutron yield. The best setup configuration defined by proton energy, foil thickness, and the angular aperture strongly depend on the performance of the accelerator as well as on the cross section of the measured sample and the requested uncertainty.

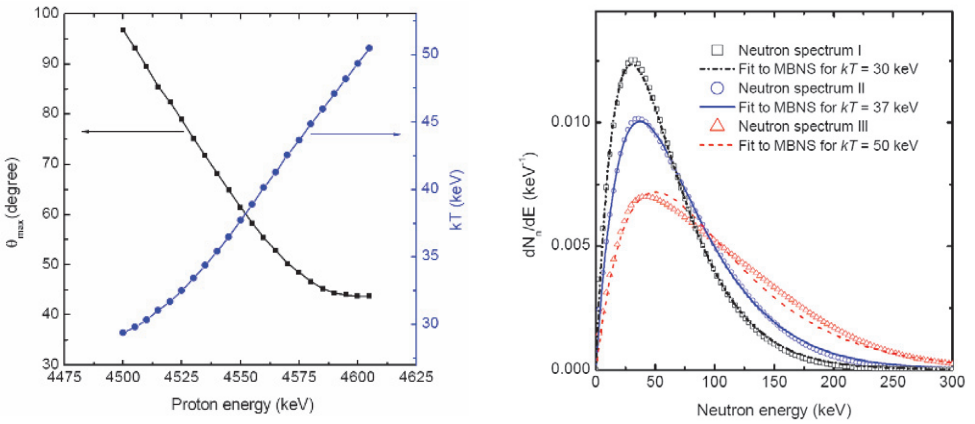

Figure 9 Left: combination of proton energy, neutron angular aperture sustained by the measuring sample and stellar energy of the Maxwellian best fit. Right: three simulated neutron spectra and Maxwellian fits corresponding to left figure.

Conclusions

Development of the LENOS facility is on-going. A proposed energy-tuning method has been investigated in-depth: different setups are proposed that should result in high quality Maxwell-Boltzmann distributions at energies ranging from kT=25 to 60 keV. The experimental validation is scheduled for March 2012. The challenging lithium metal target, based on micro channel cooling system, has been designed and constructed. The preliminary tests are very promising, suggesting that a specific power higher than 3.5 kW/cm^2 can be dissipated keeping the surface temperature of lithium well below the melting point. The liquid metal cooling system of the target based on micro channel will be implemented in 2012; we expect a further improvement of about a factor of 3 in higher specific power. A series of complementary measurements are being carried out or planned at existing accelerators, mainly at the CN (LNL-INFN, Italy) and CNA (Spain). Some preliminary experimental results were presented and perspectives are very encouraging.

Acknowledgements

MP acknowledges support from Ambizione grant of the SNSF (Switzerland), NSF grants PHY 02-16783 and PHY 09-22648 (Joint Institute for Nuclear Astrophysics, JINA), EU MIRG-CT-2006-046520, and from Eurogenesis (MASCHE).

References

[1] P.F. Mastinu, G. Martín-Hernández and J. Praena, Nucl. Inst. And Methods in Physics A601 (2009) 333.
[2] E.M. Burbidge, G.R. Burbidge, W.A. Fowler and F. Holey, Rev. Mod. Phys. 29 (1957) 547.
[3] A.G.W. Cameron, Atomic Energy of Canada Limited, CRL-41 (1957).
[4] L.-S. The, M. F. El Eid, B. S. Meyer, ApJ, 655 (2007) 1058.
[5] M. Pignatari, R. Gallino, M. Heil, M. Wiescher, F. Käppeler, F. Herwig, S. Bisterzo, ApJ 710 355 (2010) 1557.
[6] C. Arlandini, F. Käppeler, K. Wisshak, ApJ. 525 (1999) 886
[7] R. Gallino, et al. ApJ 497 (1998) 388.
[8] S. Bisterzo, R. Gallino, O. Straniero, S. Cristallo, F. Käppeler, MNRAS 404 (2010) 1529.
[9] O. Straniero, R. Gallino, S. Cristallo, Nucl. Phys. A 777 (2006) 311.

[10] C.M. Raiteri, M. Busso, G. Picchio and R. Gallino, ApJ 371 (1991) 665.
[11] F. Herwig, et al., ApJ 727 (2011) 89
[12] B. S. Meyer, D. D. Clayton, L.-S. The, ApJ 540 (2000) L49
[13] F Kappeler, H Beer and K Wisshak 1989 *Rep. Prog. Phys.* **52** (1989) 945
[14] H. Beer, G. Walter, F. Käppeler, Astro. J., Part 1 (ISSN 0004-637X), vol. 389, April 20, p. 784-79, 1992.
[15] H. Beer and F. Käppeler, Physical Review C, volume 21, number 2, page 534, 1980.
[16] W. Ratynski and F. Käppeler, Physical Review C, volume 37, number 2, 1988.
[17] A.J. Koning, S. Hilaire and M.C. Duijvestijn, "TALYS- 1.0", Proceedings of the International Conference on Nuclear Data for Science and Technology - ND2007, April 22-27, 2007, Nice, France (2008). Code distributed online at http://www.talys.eu (Current version 1.4).
[18] M. Herman, R. Capote, B.V. Carlson, et al., "EMPIRE, Nuclear Reaction Code System for Data Evaluation," Nuclear Data Sheets 108, 2655 (2007). Code distributed online at http://www- nds.iaea.org/empire and http://www.nndc.bnl.gov/empire (Current version 3.1 - Rivoli).
[19] R. Capote, M. Herman, P. Oblozinsky et al., "RIPL - Reference Input Parameter library for Calculation of Nuclear Reaction and Nuclear Data Evaluation," Nuclear Data Sheets 110, 3107 (2009). Database available online at http://www-ds.iaea.org/RIPL-3.
[20] A.J. Koning et al., "Status of the JEFF nuclear data library," J. Korean Phys. Soc. 59, No. 2, 1057 (2011).
[21] K. Shibata, O. Iwamoto, T. Nakagawa, et al, "JENDL-4.0: A New Library for Nuclear Science and Engineering," J. Nucl. Sci. Technol. 48, 1 (2011).
[22] M. B. Chadwick, P. Oblozinsky, M. Herman, et al, "ENDF/B-VII.1 Nuclear Data for Science and Technology: Cross Sections, covariances, Fission Product Yields and Decay Data," Nuclear Data Sheets 112, 2887 (2011).
[23] J. Briesmeister et al, "MCNP : a general Monte Carlo code for neutron and photon transport", Technical report LA-7396-M-REV-2 (1986), Los Alamos National Laboratory, NM, USA. Distributed by RSIC and NEA data bank.
[24] S. Agostinelli, J. Allison, K. Amako, et al., "Geant4—a simulation toolkit,", Nucl. Instr. & Methods in Phys. Res. A506, 250-303 (2003).
[25] CRC, Handbook of Chemistry and Physics, edited by D. R. Lide (CRC, Boca Raton, 2002).
[26] C. Lasance and C. Moffat, Advanced high-performance cooling for electronics, Vol 11, Number 4, 2005
[27] Proposal PAC 3/11. EUFRAT. 3th Meeting of the Programme Advisory Committee, IRMM 12 November 2010.
[28] J. Praena, N. Dzysiuk, P.F. Mastinu, G. Martín-Hernández, J. M. Quesada, M. Lozano, J. Gómez-Camacho, J. García. Proceedings of XXXIII Reunión Bienal de la RSEF, Sept. 2011 (Santander, Spain), ISBN: 978-84-86116-40-8.
[29] KADoNIS v0.3 – The third update of the "Karlsruhe Astrophysical Database of Nucleosynthesis in Stars", I. Dillmann, R. Plag, F. Käppeler and T. Rauscher; online at http://www.kadonis.org